

Phorboxazoles A and B: Potent Cytostatic Macrolides from Marine Sponge *Phorbas* Sp.[†]

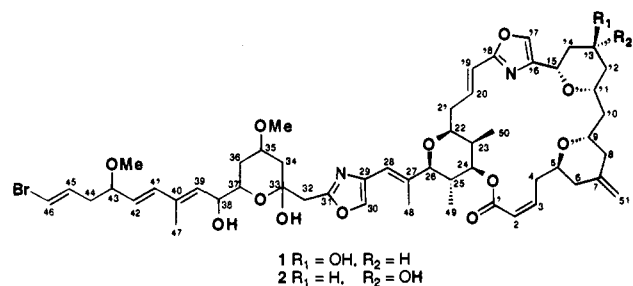
Philip A. Searle and Tadeusz F. Molinski*

Contribution from the Department of Chemistry, University of California, Davis, California 95616

Received May 2, 1995[⊗]

Abstract: Two new antifungal and cytostatic macrolides, phorboxazoles A (**1**) and B (**2**), have been isolated from the Indian Ocean marine sponge *Phorbas* sp. Structural assignment was accomplished through extensive 2D NMR spectroscopy including COSY, RCT, HMQC, and HMBC. The complete relative stereochemistry about the macrolide ring and solution conformation of **1** were established from analysis of ROESY experiments. Phorboxazoles A and B exhibit *in vitro* antifungal activity against *Candida albicans* at 0.1 $\mu\text{g}/\text{disk}$ and extraordinary cytostatic activity (mean $\text{GI}_{50} < 7.9 \times 10^{-10}$ M in the National Cancer Institute's 60 tumor cell line panel).

Cytotoxic macrolides have been isolated from a variety of sponge species. Recent examples include the exceedingly potent cytostatic agents halichondrin, spongiastatin-1¹ (=cinachyrolide²), spongiastatins 2 and 3,³ and althoyrtins A–C and desacetyl-althoyrtin A.^{4–6} The latter four compounds are structural analogs of the “spongopyran” parent skeleton while all compounds bear multiple oxane and spiroketal–oxane rings.¹ In our study of antifungal compounds from marine invertebrates, we examined an extract of the sponge *Phorbas* sp. which exhibited antifungal activity against *Candida albicans*. Bioassay-guided separation of the extract afforded two novel isomeric antifungal macrolides, phorboxazoles A (**1**) and B (**2**). Like



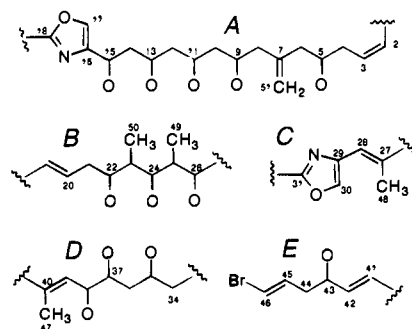
the spongiastatins, compounds **1** and **2** show exceptional cytostatic activity; however, they are the first members of a new class of macrolides with an unprecedented carbon skeleton. The phorboxazole skeleton contains 7 rings, including 2 oxazoles and 4 oxane rings, and 15 stereogenic centers, 13 of which have

been assigned relative configuration. This is only the second report of natural products from the genus *Phorbas*.⁷

Results

The methanol extract of the sponge (236 g dry weight) was subjected to a modified Kupchan solvent partition,⁸ and the CHCl_3 fraction was further separated by flash chromatography (silica gel), C_{18} reversed-phase chromatography, and HPLC (Microsorb C_{18}) to afford phorboxazole A (**1**; 95.1 mg, 0.040% dry weight) and phorboxazole B (**2**; 40.5 mg, 0.017%), both as pale yellow amorphous solids.

Phorboxazole A. The molecular formula of $\text{C}_{53}\text{H}_{71}\text{N}_2\text{O}_{13}\text{Br}$ for **1** was established by HRFABMS (m/z 1023.4243, MH^+ , Δ 2.5 mmu). The UV spectrum contained several overlapping bands at λ 235 nm ($\log \epsilon$ 4.9) indicative of conjugation. The ^1H NMR spectrum in CDCl_3 displayed well-resolved signals (Figure 1). Analysis of the COSY, long-range COSY, ^1H – ^1H relayed coherence transfer (RCT), HMQC,⁹ and HMBC¹⁰ spectra gave substructures A–E.



C2–C18: Substructure A. The largest substructure, A, was highly oxygenated and delineated by COSY and relayed coherence transfer (RCT) experiments. The ^1H NMR signals for the olefinic protons H2 and H3 were unresolved in CDCl_3 , appearing as a multiplet at δ 5.90; however, in CD_3OD , H2

(7) Rudi, A.; Stein, Z.; Green, S.; Goldberg, I.; Kashman, Y.; Benayahu, Y.; Schleyer, M. *Tetrahedron Lett.* **1994**, *35*, 2589–2592.

(8) Kupchan, S. M.; Britton, R. W.; Ziegler, M. F.; Sigel, C. W. *J. Org. Chem.* **1973**, *38*, 178–179.

(9) Bax, A.; Griffey, R. H.; Hawkins, B. L. *J. Am. Chem. Soc.* **1983**, *105*, 7188–7190.

(10) Bax, A.; Summers, M. F. *J. Am. Chem. Soc.* **1986**, *108*, 2093–2094.

* To whom correspondence should be addressed. Tel.: (916) 752-6358. FAX: (916) 752-8995.

[†] In memory of Matt Suffness, National Cancer Institute, 12/15/42 to 6/14/95.

[⊗] Abstract published in *Advance ACS Abstracts*, July 15, 1995.

(1) Pettit, G. R.; Cichacz, Z. A.; Gao, F.; Herald, C. L.; Boyd, M. R.; Schmidt, J. M.; Hooper, J. N. *J. Org. Chem.* **1993**, *58*, 1302–1304.

(2) Fusetani, N.; Shinoda, K.; Matsunaga, S. *J. Am. Chem. Soc.* **1993**, *115*, 3977–3981.

(3) Pettit, G. R.; Cichacz, Z. A.; Gao, F.; Herald, C. L.; Boyd, M. R. *J. Am. Chem. Soc., Chem. Commun.* **1993**, 1166–1168.

(4) Kobayashi, M.; Aoki, S.; Sakai, H.; Kawazoe, K.; Kihara, N.; Sasaki, T.; Kitagawa, I. *Tetrahedron Lett.* **1993**, *34*, 2795–2798.

(5) Kobayashi, M.; Aoki, S.; Sakai, H.; Kihara, N.; Sasaki, T.; Kitagawa, I. *Chem. Pharm. Bull.* **1993**, *41*, 989–991.

(6) Kobayashi, M.; Aoki, S.; Kitagawa, I. *Tetrahedron Lett.* **1994**, *35*, 1243–1246.

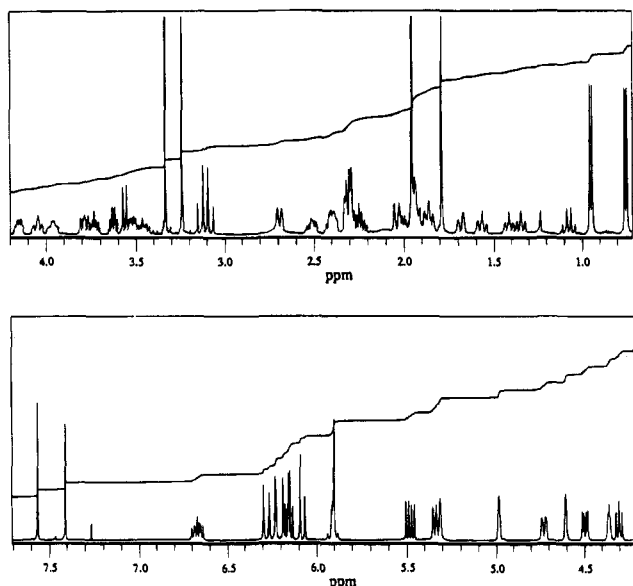


Figure 1. ^1H NMR spectrum of phorboxazole A (1), CDCl_3 , 500 MHz.

and H3 were readily distinguished (δ 5.96, ddd, $J = 11.3, 3.0, 1.0$, H2; 6.07, ddd, $J = 11.3, 9.2, 3.5$, H3) and showed a relatively small $J_{2,3}$ coupling (11 Hz) consistent with a (*Z*)-olefin. The COSY spectrum (CDCl_3) showed the signal at δ 5.90 to be coupled to both of the highly anisochronous methylene protons H4a,b (δ 2.30, m; 3.46, m) which coupled in sequence to an oxymethine H5 (δ 4.15) and methylene protons H6a,b (δ 2.04, br d, $J = 13.2$ Hz; 2.40, m). The H6 proton signals were allylically coupled to an exocyclic methylene group H51a,b (δ 4.60, br s; 4.98, br s) which was flanked by another methylene H8a,b (δ 1.86, m; 2.69, br d, $J = 11.9$ Hz). The sequence C8–C15 was comprised of a tetrad of alternating methylene and oxymethine groups, terminated by a 2,4-disubstituted oxazole, the latter evidenced by the presence of benzylic coupling ($J < 1$ Hz) between H15 (δ 4.72, dd, $J = 10.8, 2.9$ Hz) and an oxazole signal H17 (δ 7.40, s, $^1J_{\text{C-H}} = 205$ Hz).

C19–C26: Substructure B. Determination of the segment inclusive of H20 to H26 was made by combined analysis of COSY, RCT, and HMBC spectra. The protons H19 and H20 comprised a disubstituted (*E*)-olefin ($J_{19,20} = 16.0$ Hz), with H20 sequentially coupled to methylene protons H21 (δ 2.40, m, 1H; 2.51, ddd, 1H, $J = 12.7, 9.7, 5.3$ Hz) and an oxymethine H22 (δ 3.52) which in turn correlated to a methine proton H23 at δ 2.30. H23 is in turn coupled to a methyl doublet (δ 0.95) and an oxygenated methine H24 (δ 4.49). Although the H23 signal (δ 2.30) was severely overlapped by other signals, RCT correlations were observed from H22 to the methyl doublet signal H50 (δ 0.95, d, $J = 6.8$ Hz) and from H24 (δ 4.49, dd, $J = 11.2, 4.4$ Hz) to H50. H24 was further coupled to a methine proton H25 (δ 2.01) and the latter correlated to another methyl doublet signal H49 (δ 0.75, d, $J = 6.4$ Hz) and an oxymethine H26 (δ 3.56). This connection was supported by RCT correlations H49–H24 and H49–H26.

C27–C31: Substructure C. In the COSY spectrum the olefinic proton H28 (δ 6.22, bs) showed fine long range coupling ($J < 1$ Hz) to both a vinylic methyl group H48 (δ 1.96, br s) and a second oxazole singlet H30 (δ 7.56, s, $^1J_{\text{C-H}} = 208$ Hz). The C48 chemical shift (δ 14.19, q) was consistent with an (*E*)-trisubstituted olefin.¹¹

C34–C40: Substructure D. In the COSY spectrum, the C34 methylene protons (δ 1.34, 2.30) were correlated to an oxygenated methine (δ 3.74) which was in turn coupled to a methylene at C36 (δ 1.07, 1.95). These methylene protons were

in turn correlated to an oxygenated methine H37 (δ 3.79) which coupled to another oxygenated methine H38 (δ 4.30). H38 coupled to an olefinic proton (δ 5.34) which showed allylic coupling to a methyl group (δ 1.79). (*E*)-Geometry for the C39–C40 olefin was implied by the upfield ^{13}C chemical shift for the vinyl methyl group (C47, δ 13.42, q).¹¹

C41–C46: Substructure E. Connectivities from C41 to C46 were revealed by examination of the COSY spectrum. (*E*)-Olefinic protons H42 and H43 ($J_{41,42} = 15.7$ Hz) were coupled to an oxymethine (δ 3.63) which was sequentially connected to methylene protons H44 (δ 2.24, 2.30) followed by vinyl protons H45 (δ 6.15, ddd) and H46 (6.07, ddd) of an (*E*)-olefin ($J_{45,46} = 13.6$ Hz). The ^{13}C chemical shift for C46 (δ 106.35) and comparison with model compounds¹² allowed placement of the bromine at C46 as a terminal vinyl bromide. It is noteworthy that C46, C45, and C44 showed relatively intense ^{13}C NMR signals due to enhanced scalar relaxation through the nearby $^{79}\text{Br}/^{81}\text{Br}$ nucleus.^{13,14}

Assembly of Substructures. Assembly of the substructures through nonprotonated carbons was established through the HMBC data (Table 1).¹⁵ An α,β -unsaturated ester (ν 1718 cm^{-1}) was located by correlation of H2 and H3 (overlapped, δ 5.90, m, 2H) to carbonyl group C1 (δ 165.58, s), a methylene group C4 (δ 30.44, t) and oxymethine C5 (δ 73.45, d). Fragment C5 to C15 was accommodated, on the basis of HMBC correlations H5–C9 and H15–C11, by two oxane rings joined by a methylene group at C10. The oxazole proton H17 (δ 7.40, s) showed a correlation to both C16 and C18, and with assignment of these two carbons, comparison with ^{13}C data for other substituted oxazoles,¹⁶ in particular one-bond J_{CH} coupling constants,¹⁷ confirmed a second 2,4-disubstituted oxazole group. The downfield oxazole signal C18 (δ 161.28, s) showed long-range heteronuclear correlation (HMBC) to *E*-disubstituted vinyl group signals H19 (δ 6.28, d, $J = 16.0$ Hz) and H20 (δ 6.66, ddd, $J = 16.0, 9.7, 6.4$ Hz) and allowed attachment of substructures A and B as shown. Extensive HMBC correlations from H26 to C27, C28, and C48 and from H48 to C26 connected partial structures B and C. The second oxazole proton signal H30 showed HMBC correlations to C29 and C31, consistent with a 2,4-substituted oxazole while C31 correlated to an isolated methylene group H32a,b (AB quartet, δ 3.08, 3.14, $J_{\text{gem}} = 15.4$ Hz). In turn, H32a,b correlated to a quaternary carbon at δ 96.61 assigned to the hemiketal carbon C33 which was linked to adjacent methylene protons H34a,b, thus linking substructures C with D. The final substructure was attached via two- and three-bond HMBC correlations from H47 to C39, C40, and C41 and from H41 to C39 and C47. Three oxane rings were located within the fragment C5–C26. ^1H – ^1H coupling constants were consistent with the axial and equatorial couplings of one *trans*- and two *cis*-fused oxane rings at C5–C9, C11–C15, and C22–C26, respectively (see Stereochemistry section). The three oxane rings were confirmed by observation of HMBC correlations from H5 to C9 and from H15 to C11 and a weak correlation from H26 to C22. The fourth oxane

(11) Couperas, P. A.; Clague, A. D. H.; Dongen, J. P. C. M. *Org. Magn. Reson.* **1976**, *8*, 426–431.

(12) Patil, A. D.; Kokke, W. C.; Cochran, S.; Francis, T. A.; Tomszek, T.; Westley, J. W. *J. Nat. Prod.* **1992**, *55*, 1170–1177.

(13) Norton, R. S.; Croft, K. D.; Wells, R. J. *Tetrahedron* **1981**, *37*, 2341–2349.

(14) Wehrli, F. W.; Marchand, A. P.; Wehrli, S. *Interpretation of Carbon-13 NMR Spectra*; Wiley: Chichester, 1983; pp 58–62.

(15) For the assignment of nonequivalent methylene protons, Ha refers to the higher field proton, while Hb refers to the lower field proton.

(16) Adamczeski, M.; Quiñoa, E.; Crews, P. *J. Am. Chem. Soc.* **1988**, *110*, 1598–1602.

(17) Maryanoff, C. A. In *The Chemistry of Heterocyclic Compounds*; Turchi, I. J., Ed.; Wiley: New York, 1986; Vol. 45, pp 343–360.

Table 1. ^1H NMR and ^{13}C NMR Chemical Shifts^a and HMBC and ROESY Correlations^b of Phorboxazole A (1)

no.	^{13}C NMR δ (mult)	^1H NMR δ (mult, J (Hz), (int)	HMBC correlations	ROESY correlation
1	165.58 (s)			
2	120.97 (d)	5.90 (m, 1H)	C1, C4	
3	144.40 (d)	5.90 (m, 1H)	C1, C4, C5	H4a, H5, H6a
4a	30.44 (t)	2.30 (m, 1H)		H3, H4b, H5 H4a, H9
4b		3.46 (m, 1H)	C2, C3	
5	73.45 (d)	4.15 (br ddd, 11.9, 5.0, 5.0, 1H)	C7, C9	H3, H4a, H6a, H6b
6a	36.92 (t)	2.04 (br d, 13.2, 1H)	C7, C8, C51	H3, H5, H6b, H51a
6b		2.40 (m, 1H)		H5, H6a, H8a
7	141.66 (s)			
8a	38.94 (t) ^a	1.86 (m, 1H)		H6b, H8b
8b		2.69 (br d, 11.9, 1H)	C6, C7, C51	H8a, H9, H11, H51b
9	69.10 (d)	3.96 (dddd, 10.4, 10.2, 5.1, 2.5, 1H)		H4b, H8b, H10b
10a	41.24 (t)	1.41 (ddd, 13.2, 10.2, 3.1, 1H)	C9	H10b, H11
10b		1.86 (m, 1H)		H9, H10a, H12a
11	68.60 (d)	4.05 (br ddd, 11.4, 11.4, 3.2, 1H)		H8b, H10a, H12b, H15
12a	38.96 (t) ^a	1.56 (ddd, 13.6, 11.4, 2.7, 1H)	C11	H10b, H12b, H13
12b		1.68 (bd, 13.6, 1H)	C13, C14	H11, H12a, H13
13	64.28 (d)	4.36 (m, 1H)	C11, C15	H12a, H12b, H14
14a,b	34.93 (t)	1.95 (m, 2H)		H13, H15, H17
15	66.91 (d)	4.72 (dd, 10.8, 2.9, 1H)	C11, C13, C16, C17	H11, H14
16	142.08 (s)			
17	133.71 (d) ^b	7.40 (s, 1H) ^d	C16, C18	H14
18	161.28 (s)			
19	119.29 (d)	6.28 (d, 16.0, 1H)	C18, C21	H22, H50
20	134.07 (d)	6.66 (ddd, 16.0, 9.7, 6.4, 1H)	C18, C21	H21a, H21b, H22, H23, H50, H51b
21a	34.32 (t)	2.40 (m, 1H)		H20, H21b, H50
21b		2.51 (ddd, 12.7, 9.7, 5.3, 1H)	C19, C20	H20, H21a, H22
22	77.98 (d)	3.52 (ddd, 11.1, 5.3, 1.0, 1H)	C50	H19, H20, H21b, H23, H24
23	32.50 (d)	2.30 (m, 1H)		H20, H22, H24, H50
24	79.28 (d)	4.49 (dd, 11.2, 4.4, 1H)	C1, C49, C50	H22, H23, H26, H49
25	31.67 (d)	2.01 (m, 1H)	C24, C26	H49, H50
26	89.15 (d)	3.56 (d, 10.1, 1H)	C22, C27, C28, C48	H24, H28, H49
27	137.94 (s)			
28	118.47 (d)	6.22 (s, 1H)	C26, C27, C30, C48	H26, H30, H49
29	137.48 (s) ^c			
30	135.89 (d)	7.56 (s, 1H) ^e	C29, C31	H28, H48
31	160.03 (s)			
32a	39.71 (t)	3.08 (d, 15.4, 1H)	C31, C33	H34a, 33-OH
32b		3.14 (d, 15.4, 1H)	C31, C33	H34a, 33-OH
33	96.61 (s)			
34a	40.40 (t)	1.34 (ddd, 11.8, 11.8, 1.6, 1H)	C33, C35	H32a, H32b, H34b, H36a
34b		2.30 (m, 1H)		H34a, H35, 35-OMe
35	73.00 (d)	3.74 (dddd, 11.8, 11.8, 4.6, 4.6, 1H)		H34b, H36b, 35-OMe
36a	33.02 (t)	1.07 (ddd, 12.0, 11.8, 11.8, 1H)	C35, C38	H34a, H36b, H38
36b		1.95 (m, 1H)		H35, H36a, H37, 35-OMe
37	72.45 (d)	3.79 (ddd, 12.0, 7.9, 2.0, 1H)	C38, C39	H36b, H47, 33-OH
38	70.85 (d)	4.30 (dd, 9.0, 7.9, 1H)	C37, C39, C40	H36a, H41, H47
39	129.87 (d)	5.34 (d, 9.0, 1H)	C37, C41, C47	H41, H47
40	137.50 (s) ^c			
41	136.96 (d)	6.17 (d, 15.7, 1H)	C39, C47	H38, H39, H47, 43-OMe
42	128.87 (d)	5.48 (dd, 15.7, 7.9, 1H)	C40, C43, C44	H44a, H47, 43-OMe
43	81.06 (d)	3.63 (ddd, 7.9, 6.0, 5.7, 1H)	C41, C44, C45, OMe	H47, 43-OMe
44a	39.18 (t)	2.24 (dddd, 14.5, 7.1, 5.7, 1.1, 1H)	C42, C43, C45, C46	H42
44b		2.30 (m, 1H)		
45	133.66 (d) ^b	6.15 (ddd, 13.6, 7.1, 7.1, 1H)	C43, C46	
46	106.35 (d)	6.07 (ddd, 13.6, 1.1, 1.1, 1H)	C44, C45	
47	13.42 (q)	1.79 (s, 3H)	C39, C40, C41	H37, H38, H39, H41, H42, H43
48	14.19 (q)	1.96 (s, 3H)	C26, C27, C28	H30
49	13.28 (q)	0.75 (d, 6.4, 3H)	C24, C25, C26	H24, H25, H26, H28
50	5.98 (q)	0.95 (d, 6.8, 3H)	C22, C23, C24	H19, H20, H21a, H23, H25, H51a, H51b
51a	110.08 (t)	4.60 (br s, 1H)	C6, C8	H6a, H50, H51b
51b		4.98 (br s, 1H)	C6, C8	H8b, H20, H50, H51a
35-OMe	55.74 (q)	3.34 (s, 3H)	C35	H34b, H35, H36b
43-OMe	56.34 (q)	3.24 (s, 3H)	C43	H41, H42, H43
33-OH		5.31 (s, 1H) ^f		H32a, H32b, H37

^{a-c} Assignments interchangeable. ^d $^1J_{\text{CH}} = 205$ Hz. ^e $^1J_{\text{CH}} = 208$ Hz. ^f Remaining OH signals; 2.10 (br s, 1H), 2.71 (br s, 1H). ^g Recorded in CDCl_3 at 500 MHz (^1H) and 100 MHz (^{13}C). ^h HMBC optimized for $^2J_{\text{CH}} = 10$ Hz. ROESY mixing time t_m 500 ms.

ring was revealed by NOE from 33-OH to H37 across the oxygen bridge (see stereochemistry). The positions of the two methoxyl groups were located on C43 and C35 on the basis of HMBC correlations to these carbons, leaving two free hydroxyl groups at C13 and C38. Finally, HMBC showed a three-bond correlation between the ester oxymethine H24 (δ 4.49,

dd) and carbonyl C1 (δ 165.58, s), thus closing the macrolide ring. Attempts to acetylate **1** (Ac_2O , py, 23 °C) to confirm the hydroxyl group placements resulted in extensive decomposition of the molecule.

Stereochemistry. Relative stereochemistry was determined through analysis of ^1H – ^1H coupling constants and ROESY data

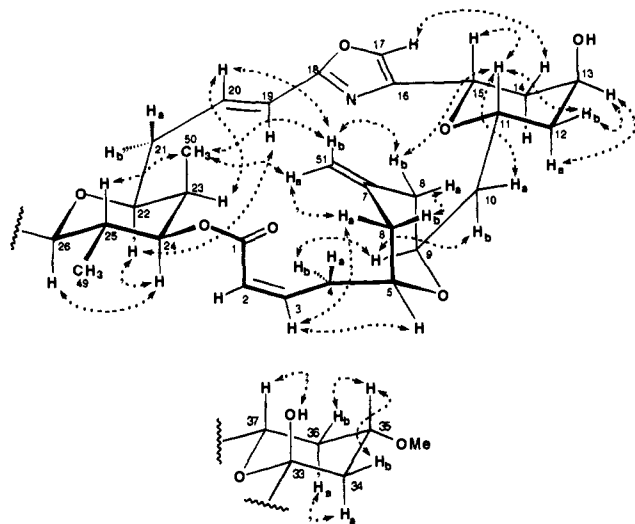


Figure 2. Summary of ROESY correlations observed for phorboxazole A (**1**), t_m 500 mS, CDCl_3 . Geminal and some vicinal correlations omitted for clarity.

(Figure 2) and was analyzed independently for each molecular fragment and finally linked to provide configurational assignment about the large ring.

(a) C33–C37 Fragment. A large coupling (12.0 Hz) between H37 and H36a indicated a diaxial arrangement for these protons. H35 was also assigned as axial on the basis of large couplings (11.8 Hz) to both H34a and H36a. The ketal hydroxyl group was established as being in an axial position due to observation of a small w-coupling to H34a and a ROESY correlation to H37.

(b) C22–C26 Fragment. A large coupling ($J = 10.1$ Hz) between H26 and H25 indicated a diaxial arrangement for these protons and an equatorial methyl group (H49). The other methyl group (H50) was assigned as axial due to observation of a ROESY correlation to H25 and the particularly upfield ^{13}C NMR chemical shift for C50 (δ 5.98).¹⁴ H24 exhibited a large coupling (11.2 Hz) to H25 and ROESY correlations to H22 and H26; thus, both H24 and H22 are in axial positions.

(c) C5–C15 Fragment. An axial position for H15 was evident from the large coupling (10.8 Hz) to H14 and a ROESY correlation to an axial H11, with H11 exhibiting a large coupling (11.4 Hz) to H12a. H13 showed only a small coupling (2.7 Hz) to H12a and was assigned an equatorial position. The stereochemistry of the C11–C15 ring could be correlated to that of the second ring C5–C9 through the methylene bridge C10 (Figure 2). H11 exhibited a large coupling (11.4 Hz) to H10b and showed a ROESY correlation to only H10a, indicating an *anti* arrangement of H11 and H10b. A large coupling between H10a and H9 and a ROESY correlation between H10b and H9 indicated that H9 and H10a were also in a diaxial arrangement. H9 also exhibited a large coupling (10.2 Hz) to H8a and thus occupies an axial position on the ring. A ROESY correlation between H6b and H8a confirmed axial positions for these two protons, while H6a and H8b showed ROESY correlations to H51a and H51b, respectively, indicating the chair conformation depicted in Figure 2. H5 occupied an equatorial position, as evident from the small couplings to both H6a and H6b. The axial position of C4 was also confirmed by a ROESY correlation from H4b to H9.

(d) Complete Macrolide Ring. Simultaneous assignment of *both* conformation and relative configuration in novel medium- and large-ring substituted macrolides is seldom possible due to lack of a sufficient number of independent variables and interruption of the carbon chain by quaternary

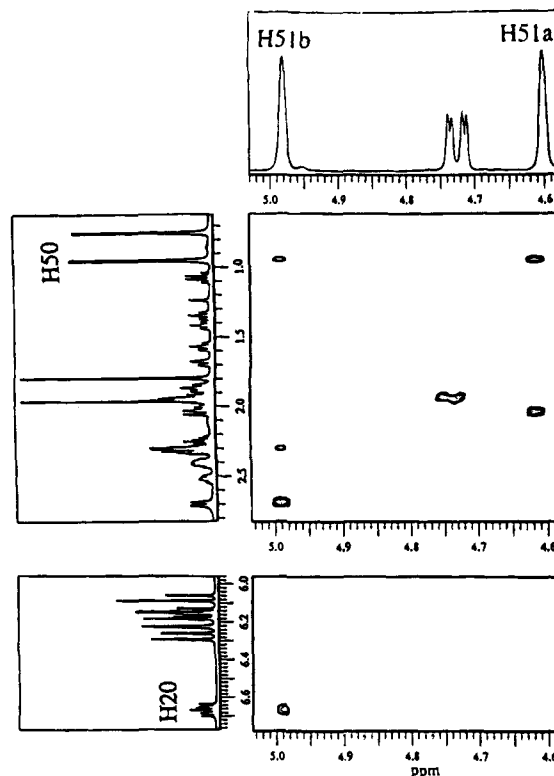


Figure 3. Expansion of the ROESY spectrum of **1** (t_m 500 mS, CDCl_3) showing transannular NOEs. Only negative contours shown.

carbons. An exception was found in the case of **1** due to the conformational restrictions imposed by the presence of three oxane rings and one oxazole along the perimeter of the macrolide annulus. From examination of coupling constants and NOE studies, compound **1** appears to be a relatively rigid ring. Measurement of NOESY spectra gave few useful cross peaks; however, the ROESY spectrum (500 MHz, CDCl_3 , t_m 500 ms) provided a rich data set of correlations, allowing assignment of the relative stereochemistry between the two sections of the macrolide ring, C5–C15 and C22–C26 (Figures 2 and 3). Because the relative configurations internal to each oxane ring (*ax*–*eq*) were determined, it only remained to examine all possible combinations of oxane ring stereochemistries that would fit the NOE constraints. Analysis of Dreiding molecular models revealed, that of the four possible arrangements of the macrolide ring of **1**, only the combination of oxane relative stereochemistries depicted in Figure 2 would account for observed ROESY correlations between H51 and H50–H20 (contacts $< 4 \text{ \AA}$) and satisfy NOEs observed (H8_{eq} to H11_{ax}) between oxane rings C11–C15 and C5–C9. All ROESY correlations were in full agreement with the assigned stereochemistry and 3D solution structure. Understandably, the relative stereochemistry between the macrolide ring and the C33–C37 oxane ring could not be established, although vicinal coupling constants and ROESY showed it was *cis*-substituted at C33 and C37 with an axial hemiketal OH as expected from the anomeric effect. The configurations of C38 and C43 remain unassigned, as does the absolute configuration of **1**.

The solution structure of the phorboxazole molecule reveals an interesting topology that results from a relatively rigid macrolide ring and a *trans*-fused C5–C9 oxane ring which places the exocyclic methylene C51 directly above the center of the macrolide ring. The molecule thus adopts a “capped annulus” or bowl-shaped conformation with entry to the macrolide ring blocked from one face.

Phorboxazole B. Phorboxazole B (**2**, $\text{C}_{53}\text{H}_{71}\text{N}_2\text{O}_{13}\text{Br}$) is isomeric with **1** (m/z 1023.4271, MH^+ , Δ 6.3 mmu). Com-

parison of the ^1H NMR and ^{13}C NMR spectra of phorboxazole B (**2**) showed almost identical features. The only chemical shift differences were observed in substructure A. Careful analysis of ^1H vicinal coupling constants of protons neighboring H13 revealed that the multiplet pattern of H13 was now different and included two diaxial vicinal couplings (H14a, δ 1.63, br ddd, $J = 11.6, 11.6, 11.6$ Hz), consistent with an equatorial C13 hydroxyl group. ROESY correlations were observed from H13 to H15ax and H11ax, but otherwise the ROESY map of **2** was identical to that of **1**. Therefore, phorboxazole B is the C13 epimer of **1**.

Discussion

Only one report has appeared describing natural products from the genus *Phorbas*, four phenylpyrrolyloxazoles named phorboxazoles A–D.⁷ A steadily increasing family of oxazole-containing compounds have been isolated from marine invertebrates over the past decade. For example, the molecular structures of ulapualides A and B,¹⁸ kabiramides B and C,¹⁹ halichondramides,¹⁹ mycalolides,²⁰ and jaspisamides²¹ isolated from sponges or the nudibranch *Hexabranchnus sanguineus* each contain a distinctive contiguous trisoxazole moiety. Less frequently encountered bisoxazoles are represented by bengazoles A and B, reported by Crews *et al.*,¹⁶ bengazoles B1 and C–G reported by our group,²² several related C10 desoxybengazoles,^{23,24} and hennoxazole, reported by Scheuer *et al.*²⁵ and recently synthesized by Wipf and co-workers.²⁶ The theonzolides A–C^{27,28} are interesting macrolides containing a thiazole–oxazole combination. Although kabiramide and theonzolide classes of macrolides also embody oxazole units, the phorboxazoles are structurally unrelated and compounds **1** and **2** represent a new class of macrolides containing an unprecedented oxazole–trisoxane fused ring system.

Biological Activity. Compounds **1** and **2** exhibited potent activity against *C. albicans*, but showed no ergosterol dependence.²⁹ Phorboxazole A (**1**) gave the following zones of inhibition in the agar disk diffusion assay: 12 mm (loading, 1 μg) and 9 mm (0.1 μg). Phorboxazole B (**2**) was marginally less active: 11 mm (1 μg) and 8 mm (0.1 μg). Both compounds were also active against *Saccharomyces carlsbergensis*: **1**, 20 mm (1 μg) and 13 mm (0.1 μg); **2**, 16 mm (1 μg) and 10 mm (0.1 μg). Neither compound showed antibacterial activity against *Escherichia coli*, *Pseudomonas aeruginosa*, or *Staphylococcus aureus* in agar disk diffusion assays. Replicate testing of **1** and **2** in the National Cancer Institute's panel of 60 tumor cell lines^{30,31} showed exceptional inhibition of cell growth. Both

compounds gave mean GI_{50} 's $< 7.9 \times 10^{-10}$ M; however, most cell lines were still 100% inhibited at this, the lowest, test concentration. Compounds **1** and **2** thus show activity on the same order of magnitude reported for spongistatin-1¹ and are among the most potent cytostatic agents yet discovered. Pettit has commented on the empirical correlation of molecular structures bearing multiple oxane and spiroketal rings in macrolides and polyethers from marine invertebrates with exceptional cell growth inhibitory activity.³² Further biological evaluation of **1** and **2** is in progress, and full results will be reported in due course.

Experimental Section

General Procedures. General procedures can be found elsewhere.³³ Mass spectra were provided by the University of Minnesota Chemistry Department Mass Spectrometry Service Laboratory.

NMR Spectroscopy. NMR spectra were measured at 300 or 500 MHz (^1H) and 75.4, 100, or 125 MHz (^{13}C). ^1H NMR and ^{13}C NMR are referenced to CDCl_3 solvent signals at 7.26 and 77.00 ppm, respectively. Multiplicities of ^{13}C spectra were assigned by DEPT experiments. Standard pulse sequences were employed for DEPT and magnitude COSY, LRCOSY, RCT, and HETCOR. Phase sensitive ROESY spectra were measured with a mixing time t_m of 500 ms, while HMQC and HMBC were optimized for $^1J_{\text{C-H}} = 140$ Hz and $^2\text{-}^3J_{\text{C-H}} = 10$ Hz, respectively.

Isolation. The sponge (93-05-054) was collected in January 1993 by hand using SCUBA near Muiron Island (21° 40' S, 114° 18' E), Western Australia. The animals were immediately frozen at -20°C until required. The sponge sample, described by John Hooper, Queensland Museum, Brisbane, Australia, is a new species of *Phorbas* (see supporting information). A voucher specimen is archived at the Queensland Museum (QM G304923). Lyophilized animals (236 g) were extracted with MeOH (3 \times 2 L) and filtered. The extracts were combined, concentrated to approximately 300 mL, and successively extracted using a modified Kupchan partition⁸ as follows. The water content (% v/v) of the MeOH extract was adjusted prior to sequential partitioning against *n*-hexane (10% v/v H_2O), CCl_4 (20%), and CHCl_3 (40%). The aqueous phase was concentrated to remove MeOH and then extracted with *n*-BuOH. The CHCl_3 (2.19 g) extract was fractionated by flash chromatography on silica gel (stepwise gradient elution, $\text{CHCl}_3/\text{MeOH}$ (99:1) to 100% MeOH), followed by reversed-phase chromatography (C_{18} silica cartridge, MeOH/ H_2O (9:1)) and HPLC (Microsorb C_{18} column, 10 \times 300 mm, MeOH/ H_2O (82:18)) to afford **1** (95.1 mg, 0.040% dry weight of animal) and **2** (40.5 mg, 0.017%), both as pale yellow amorphous solids.

Data for Phorboxazole A (1): $\text{C}_{53}\text{H}_{71}\text{N}_2\text{O}_{13}\text{Br}$; $[\alpha]_{\text{D}} + 44.8^\circ$ (c 1.0 MeOH); UV (MeOH) λ_{max} 235 nm ($\log \epsilon$ 4.9); IR (film) ν_{max} 3390 (br), 1718, 1188, 1158, 1089, 731 cm^{-1} ; ^1H and ^{13}C NMR see Table 1; FABMS m/z 1025 (MH^+ , ^{81}Br , 100%), 1023 (MH^+ , ^{79}Br , 100%), 1007 ($\text{MH}^+ - \text{H}_2\text{O}$, ^{81}Br , 57%), 1005 ($\text{MH}^+ - \text{H}_2\text{O}$, ^{79}Br , 55%); HRFABMS found m/z 1023.4243 (MH^+), $\text{C}_{53}\text{H}_{72}\text{N}_2\text{O}_{13}\text{Br}$ requires 1023.4218.

Data for Phorboxazole B (2): $\text{C}_{53}\text{H}_{71}\text{N}_2\text{O}_{13}\text{Br}$; $[\alpha]_{\text{D}} + 44.4^\circ$ (c 1.0 MeOH); UV (MeOH) λ_{max} 235 nm ($\log \epsilon$ 4.8); IR (film) ν_{max} 3390 (br), 1718, 1192, 1158, 1089, 731 cm^{-1} ; ^1H and ^{13}C NMR see Table 1; FABMS m/z 1025 (MH^+ , ^{81}Br , 100%), 1023 (MH^+ , ^{79}Br , 100%), 1007 ($\text{MH}^+ - \text{H}_2\text{O}$, ^{81}Br , 43%), 1005 ($\text{MH}^+ - \text{H}_2\text{O}$, ^{79}Br , 45%); HRFABMS found m/z 1023.4271 (MH^+), $\text{C}_{53}\text{H}_{72}\text{N}_2\text{O}_{13}\text{Br}$ requires 1023.4218.

Acknowledgment. This work was supported by the National Institutes of Health (Grant AI 31660). We are most grateful to John Hooper (Queensland Museum, Brisbane, Australia) for identification of the sponge, Mary K. Harper (Scripps Institution

(18) Roesener, J. A.; Scheuer, P. J. *J. Am. Chem. Soc.* **1986**, *108*, 846–847.

(19) Matsunaga, S.; Fusetani, N.; Hashimoto, K.; Koseki, K.; Noma, M. *J. Am. Chem. Soc.* **1986**, *108*, 847–849.

(20) Fusetani, N.; Yasumuro, K.; Matsunaga, S.; Hashimoto, K. *Tetrahedron Lett.* **1989**, *30*, 2809–2812.

(21) Kobayashi, J.; Murata, O.; Shigemori, H. *J. Nat. Prod.* **1993**, *56*, 787–791.

(22) Molinski, T. F. *J. Nat. Prod.* **1993**, *56*, 1–8.

(23) Rodríguez, J.; Nieto, R. M.; Crews, P. *J. Nat. Prod.* **1993**, *56*, 2034–2040.

(24) Rudi, A.; Kashman, Y.; Benayahu, Y.; Schleyer, M. *J. Nat. Prod.* **1994**, *57*, 829–832.

(25) Ichiba, T.; Yoshida, W. Y.; Scheuer, P. J.; Higa, T.; Gravalos, D. *J. Am. Chem. Soc.* **1991**, *113*, 3173–3174.

(26) Wipf, P.; Lim, S. *J. Am. Chem. Soc.* **1995**, *117*, 558–559.

(27) Kobayashi, J.; Kondo, K.; Ishibashi, M.; Wälchli, M. R.; Nakamura, T. *J. Am. Chem. Soc.* **1993**, *115*, 6661–6665.

(28) Kondo, K.; Ishibashi, M.; Kobayashi, J. *Tetrahedron* **1994**, *50*, 8355–8362.

(29) Antonio, J.; Molinski, T. F. *J. Nat. Prod.* **1993**, *56*, 54–61.

(30) Suffness, M.; Newman, D. J.; Snader, K. In *Bioorganic Marine Chemistry*; Scheuer, P. J., Ed.; Springer-Verlag: Berlin, 1989; Vol. 3, p 175.

(31) Boyd, M. R.; Paull, K. D.; Rubinstein, L. R. In *Antitumor Drug Discovery and Development*; Valeriote, F.; Corbett, T.; Baker, L., Eds.; Kluwer Academic: Amsterdam, 1991; pp 11–34.

(32) Pettit, G. R.; Tan, R.; Gao, R. T.; Williams, M. D.; Doubek, D. L.; Boyd, M. R.; Schmidt, J. M.; Chapuis, J.-C.; Hamel, E.; Bai, R.; Hooper, J. N. A.; Tackett, L. P. *J. Org. Chem.* **1993**, *58*, 2538–2543.

(33) Searle, P. A.; Molinski, T. F. *J. Org. Chem.* **1993**, *58*, 7578–7580.

of Oceanography) for taxonomic assistance, Ed Larka, University of Minnesota, Department of Chemistry for FABMS, and Steven Taylor and Denise C. Manker for assistance with sponge collection. We also thank Jeff S. de Ropp for assistance with the 500 MHz NMR spectra. The 500 MHz NMR spectrometer was partially funded through NIH Grant ISIO-RR04795 and NSF Grant BBS88-04739.

Supporting Information Available: Figures showing the ^1H , ^{13}C , DEPT, COSY, HETCOR, HMQC and ROESY spectra

of **1** and **2** and the RCT and HMBC spectra of **1**, a table giving complete chemical shift assignments of **2**, and text giving the taxonomic description of the sponge sample (16 pages). This material is contained in many libraries on microfiche, immediately follows this article in the microfilm version of the journal, can be ordered from the ACS, and can be downloaded from the Internet see any current masthead page for ordering information and Internet access instructions.

JA951421X